Journal of Medicinal Chemistry

Article

Cite This: J. Med. Chem. XXXX, XXX, XXX−XXX

pubs.acs.org/jmc

Development of Gleevec Analogues for Reducing Production of β-Amyloid Peptides through Shifting β-Cleavage of Amyloid Precursor Proteins

Weilin Sun, William J. Netzer, Anjana Sinha, Katherina Gindinova, Emily Chang, and Subhash C. Sinha*

Laboratory of Molecular and Cellular Neuroscience, The Rockefeller University, New York, New York 10065, United States

Supporting Information

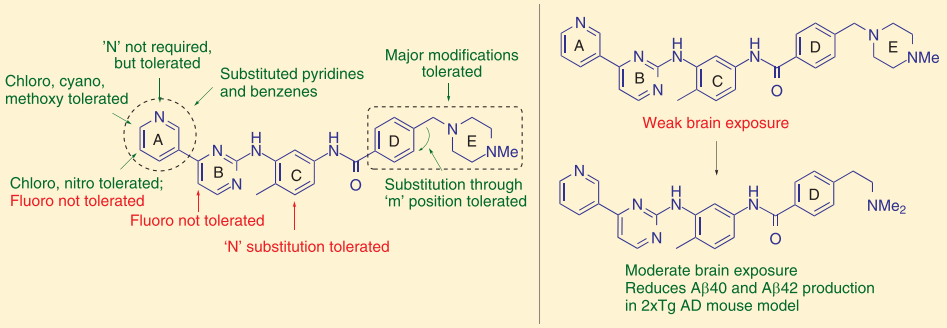

ABSTRACT: Imatinib mesylate, **1a**, inhibits production of β-amyloid (Aβ) peptides both in cells and in animal models. It reduces both the β-secretase and γ-secretase cleavages of the amyloid precursor protein (APP) and mediates a synergistic effect, when combined with a β-secretase inhibitor, BACE IV. Toward developing more potent brain-permeable leads, we have synthesized and evaluated over 75 **1a**-analogues. Several compounds, including **2a−b** and **3a−c**, inhibited production of Aβ peptides with improved activity in cells. These compounds affected β-secretase cleavage of APP similarly to **1a**. Compound **2a** significantly reduced production of the Aβ42 peptide, when administered (100 mg/kg, twice daily by oral gavage) to 5 months old female mice for 5 days. A combination of compound **2a** with BACE IV also reduced Aβ levels in cells, more than the additive effect of the two compounds. These results open a new avenue for developing treatments for Alzheimer's disease using **1a**-analogues.

1. INTRODUCTION

Neurotoxic forms of β-amyloid (Aβ) peptides that have been implicated for Alzheimer's disease (AD)[1−3] are produced by sequential cleavages of the amyloid precursor protein (APP) by β-secretase (BACE1) followed by γ-secretase (GS).[4−6] N- and C-terminal fragments, soluble APPβ (sAPPβ)[7] and β-C terminal fragment (βCTF),[8] are two other potentially neurotoxic entities produced by cleavage of APP by BACE1.[5,9] We have previously shown that imatinib mesylate (Gleevec), **1a**, which is a potent bcr-Abl kinase inhibitor,[10] and also an FDA-approved drug for the treatment of chronic myelogenous leukemia[11] and gastrointestinal stromal tumor,[12] reduces levels of Aβ peptide in cultured cells and in guinea pigs.[13] Compound **1a** lowers Aβ levels by selective, indirect reduction of both BACE and GS cleavages of full-length APP and its metabolite, APP-βCTF, respectively.[13,14] This dual targeting and secretase selectivity set **1a** apart from typical BACE and GS inhibitors (BACEi and GSi) that have failed in clinical trials.[15−18] Besides, a combination of **1a** and the potent BACEi, BACE IV, in N2a695 cells acts in a synergistic manner to lower Aβ production.[14] In a clinical setting, such a combination could reduce the side-effects of a BACEi[19] by minimizing inhibitor dosage. However, the p-glycoprotein (pGP) present at the blood−brain barrier (BBB) rapidly pumps out **1a** from the brain, thus preventing **1a** from achieving therapeutic concentration in the central nervous system.[20,21] This together with the fact that **1a** is a relatively less explored molecular entity in terms of APP metabolism prompted us to develop more potent and brain-permeable **1a**-analogues. Initially, we have prepared straight **1a**-analogues by performing simple modifications of **1a** and determined and compared their effects on Aβ production in cellular assays. We obtained dozens of compounds that show some improvement in their activities. We focused on five potent **1a**-analogues, **2a−b** and **3a−c** (Figure 1), that also accumulated moderately in wild-type mouse brain. Here, we describe the results of our studies with these compounds showing that: (1) compounds **2a−b** and **3a−c** reduce Aβ production similarly to **1a** by shifting β-cleavage of APP[14] and (2) compound **2a** reduces Aβ42 levels in 5 months old 2xTg female AD mice significantly when administered 100 mg/kg twice daily for 5 days.

Received: December 21, 2018

DOI: 10.1021/acs.jmedchem.8b02007
J. Med. Chem. XXXX, XXX, XXX−XXX

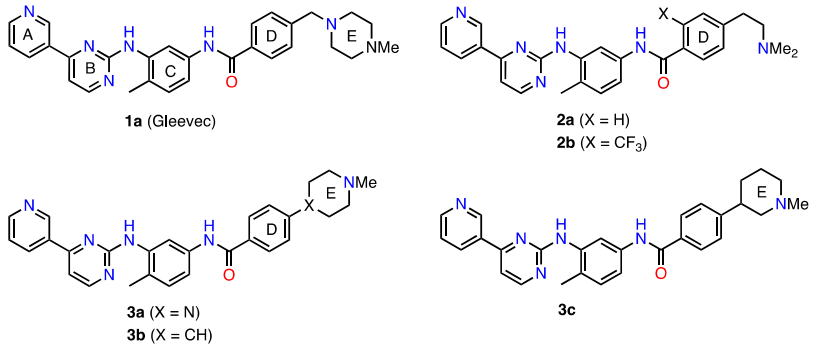

Figure 1. Structure of imatinib mesylate, **1a**, and selected potent analogues for evaluation.

Scheme 1. Development of Active 1a-analogues[a]

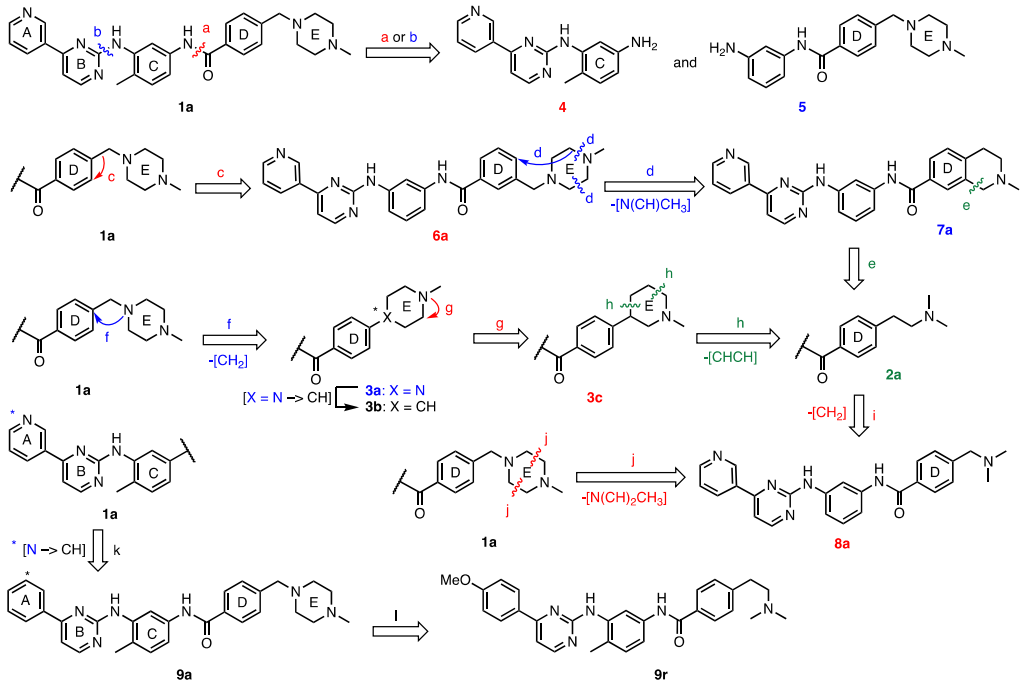

[a]Fragmentation of **1a** across "a" and "b" can afford compounds **4** and **5**. Compound **2a** can be obtained from **1a** via **6a** and **7a**, involving steps c–e or via compounds **3a–c** (steps f–h). Compound **1a** can also be modified to **8a**, which is a truncated analog of **2a**, and to **9a** and **9r**. Compound **9a** possesses an A ring modified, whereas **9r** has both A and E ring modified. Additional analogues of **9a** have one or more rings modified from A, B, and/or C ring(s), and a few of those also have an E ring modified (see: Table 2)

2. RESULTS AND DISCUSSION

Our study started with the simple modification of **1a** for identifying the molecular motifs that are required for reducing the production of secreted Aβ peptides. We prepared truncated compounds **4** and **5** (Scheme 1) containing three or four rings, and their analogs (Figure S1). Compounds **5** was previously shown to lower Aβ level more potently than **1a** in an assay performed in drosophila.[22] Because of the low molecular size and less number of hydrogen donor and acceptor atoms (N, O), such compounds could also possess greater brain permeability and retention. However, we found that all truncated **1a**-analogues, including **5**, were inactive or had lost substantial activity (see: Figure S2A). The results led us to focus on **1a**-analogues that possess all five rings of the parent compound. Thus, we made step-wise modifications in one or more rings of **1a** and prepared compounds of series **1**–**3** that possess ABC rings identical to the parent compound, **1a**. Compounds of series **2** and **3** were developed by making sequential changes in connection sites between the C/D or D/E rings in **1a**, as shown in Scheme 1, via **6a** → **7a** → **2a** → **3c** →**3b** →**3a** and via **3a** → **3b** → **3c** → **2a**.

We further modified **1a** to compounds of the **8** and **9** series, such as **8a** and **9a** or **9r** in Scheme 1. Compound **8a** closely resembles **2a**, whereas compound **9a** possesses a modified A ring. Other analogues of **9a** can have one or more of ABC rings modified, and some analogues, such as **9r** (Scheme 1) also have an E ring modified (see Table 2). Because the primary goal of this study was to identify modules that could enhance activity, majority of compounds, especially those possessing a piperazine ring in **1**–**2**, **5**–**6**, and in the **9** series can still possess pGP activity. Conversely, the parent compounds or some analogues: (1) lacking a piperazine ring in series **1** or a donor/acceptor "N"/"O" atom(s) in series **2** and **3** or (2) having less freedom of rotation across D/E rings in series **3** and **7** are likely to have lower pGP activity. Several **8**- and **9**-series compounds possessing smaller molecular size and lacking one

DOI: 10.1021/acs.jmedchem.8b02007
J. Med. Chem. XXXX, XXX, XXX–XXX

Scheme 2. General Synthesis of 1a-Analogues[a]

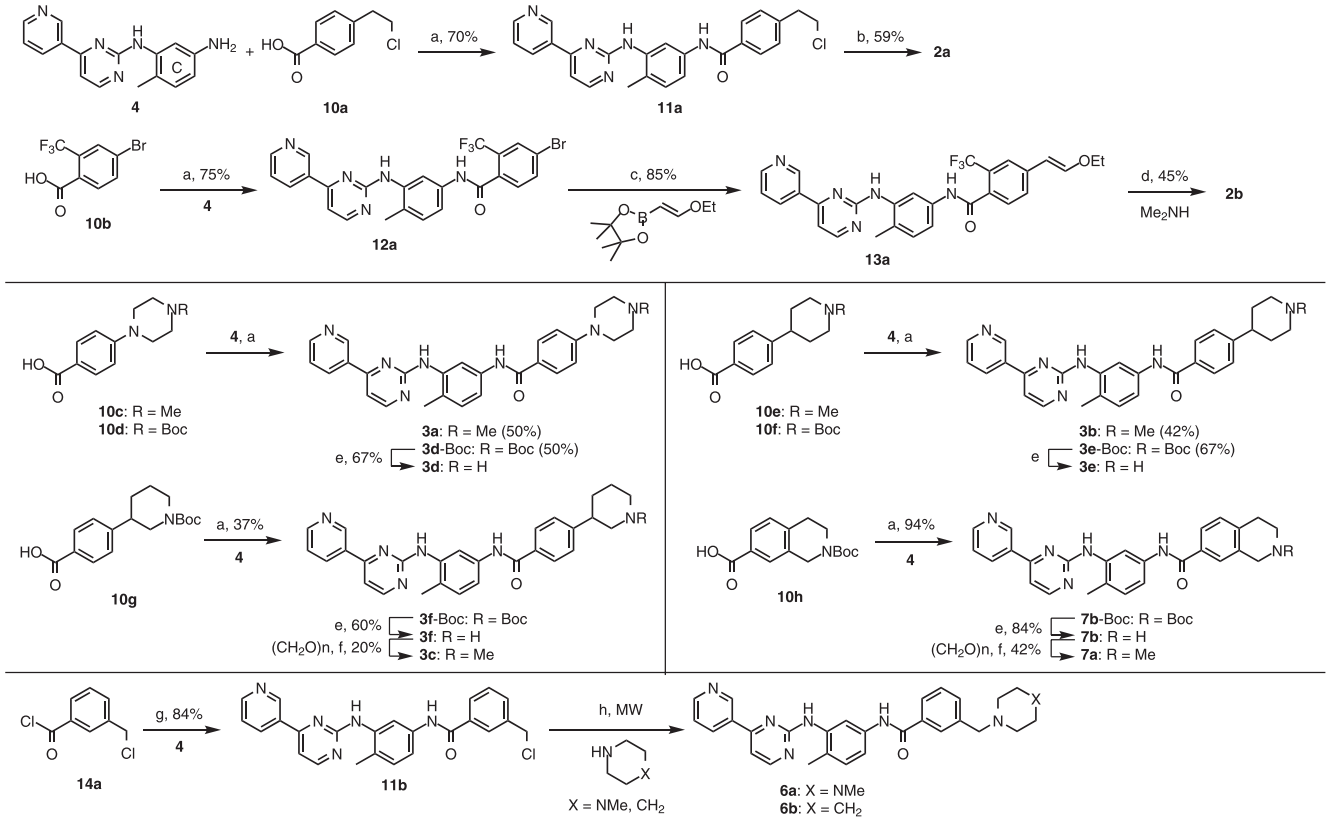

[a]Key: MW, microwave; (a) HATU, DIEA, DMF, RT, 16 h; (b) aq Me_2NH (40%, pressure bottle), 120 °C, 16 h; (c) MW, $Pd(PPh_3)_4$, aq Cs_2CO_3 (2 M), dioxane, 100 °C, 45 min; (d) (i) TFA, CH_2Cl_2, RT, 16 h, (ii) Me_2NH (2 M, THF), $NaCNBH_3$, 0 °C-RT, 16 h; (e) 4 N HCl, dioxane-EtOAc, RT, 16 h; (f) $(CH_2O)_n$, $NaCNBH_3$, 0 °C-RT, 16 h; (g) DIEA, THF, RT, 1 h; (h) MW, 100 °C, K_2CO_3, MeCN, 30 min.

or more donor/acceptor "N" atom could also possess lower pGP activity.[23]

We prepared compounds **2a–b**, **3a–f**, **6a–b**, and **7a–b** by modifying the known syntheses of compound **1a**,[24] using amine **4** and acid **10a–h** or acid chloride **14a** in 1–4 steps (Scheme 2). Thus, HATU coupling of **4** with **10a–h** or the usual amide coupling with **14a** in the presence of diisopropylethylamine (DIEA) afforded intermediates **11a–b**, **12a**, **3d**-Boc, **3e**-Boc, **3f**-Boc, and **7b**-Boc, or the target compounds **3a–b**. Homobenzyl and benzyl chloride intermediates, **11a** and **11b** were substituted with dimethylamine, *N*-methylpiperazine and piperidine to yield compounds **2a** and **6a–b**. Intermediate **12a** was converted to compound **2b** by performing Suzuki coupling[25,26] with *trans*-2-ethoxyethenyl-1-boronic acid pinacol ester,[27] followed by trifluoroacetic acid (TFA)-deprotection of the resulting vinyl ether, **13a**, to afford aldehyde and reductive amination of the latter product with dimethylamine. Boc intermediates, **3d**-Boc, **3e**-Boc, **3f**-Boc, and **7b**-Boc, were acid-deprotected to yield the target compounds, **3d–f** and **7b**. Finally, compounds **3c** and **7a** were obtained by reductive amination of **3f** and **7b** using paraformaldehyde, $(CH_2O)_n$. All **1a**-analogues, including compounds **1c–l**, **2c–j**, **3g–i**, and **6c–g**, were prepared similarly or by modifying one or more steps. We also designed and prepared compounds, **8a–q** and **9a–u**. Compounds of series **8** are nor homologs of **2a** and analogues, whereas compounds **9a–u** possess one or more rings of ABC that are different from the parent compound, **1a**, and **9r-u** also have an E ring modified. Structures of all compounds from series **1–3** and **6–9** can be found in Figure 1, Schemes 1 and 2, Tables 1 and 2.

2.1. Screening of 1a-Analogues Identified Dozens of Compounds Inhibiting Production of the Aβ Peptide in N2a695 Cells Similarly or Greater than the Parent Compound 1a. We examined all compounds using mouse neuroblastoma N2a695 cells overexpressing human APP695.[14] N2a695 cells secrete sufficient quantities of Aβ40 and Aβ42 peptides into cell culture media in 5 h to determine their concentration with high accuracy using commercially available enzyme-linked immunosorbent assay (ELISA) kits. Under these conditions, Aβ40 levels were generally reduced by 35–45% when cells were treated with 10 μM **1a** compared to a negative dimethylsulphoxide (DMSO) control. Occasionally, Aβ40 levels were found to be greater than 45% or lower than 35% under similar conditions using 10 μM **1a**, and readings for the test compounds also varied similarly. These differences may have resulted from testing cell cultures in different growth phases (i.e., logarithmic growth vs Contact-inhibited cells). The screening results for all compounds showing their effects on Aβ40 levels are shown in Figure S2. We have found as many as 44 additional compounds, in addition to compounds, **2a–b** and **3a–c**, which reduced Aβ levels by 40–70% or more. Thus, by comparing the structures of all 75 compounds (Figure 1, Schemes 1 and 2, Tables 1 and 2, and Figure S1) and the results of Aβ production, we have made the following conclusions:

First, all four ABCD rings of **1a** and an alkyl or cyclic amine are required to maintain the Aβ-lowering activity of the parent

DOI: 10.1021/acs.jmedchem.8b02007
J. Med. Chem. XXXX, XXX, XXX–XXX

Table 1. Structure of 1a-Analogues (Series 1−3 and 6) Possessing Modified DE Rings

ID	Structure	ID	Structure	ID	Structure
1b	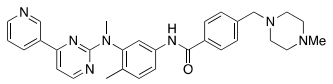	1c	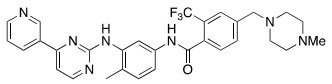	1d	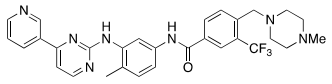
1e	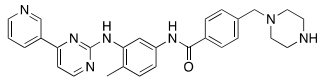	1f	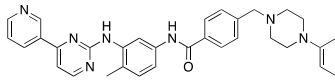	1g	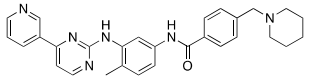
1h	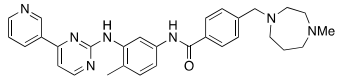	1i	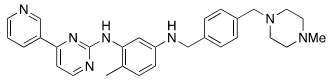	1j	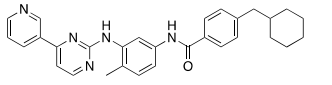
1k	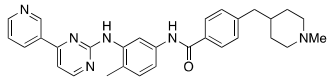	1l	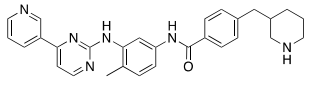	2c	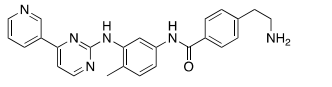
2d	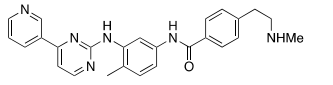	2e	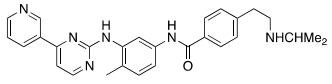	2f	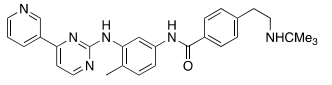
2g	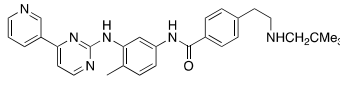	2h	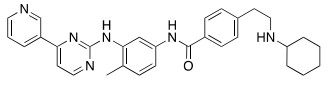	2i	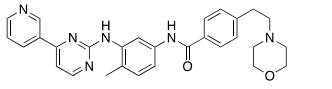
2j	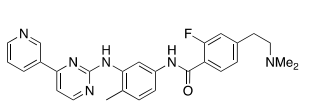	3g	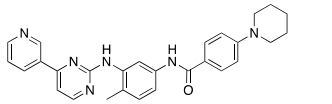	3h	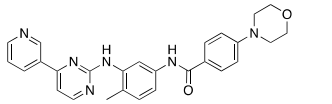
3i	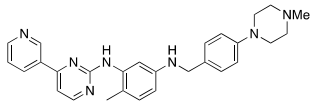	6c	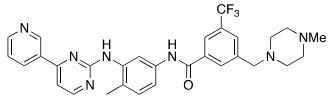	6d	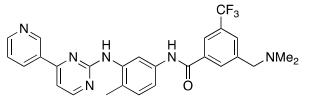
6e	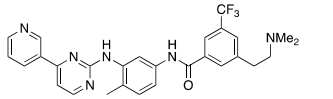	6f	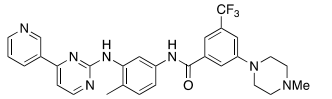	6g	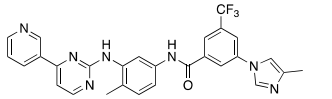

compound. This is evident from the fact that none of the compounds among **4a-h** and **5** (Figure S1) reduced Aβ levels by more than 10−20% (Figure S2A). Second, the pyridine "N" in ring "A" of **1a**-analogues, which is required in **1a** for kinase binding, is not essential for inhibiting Aβ secretion. In fact, several compounds having phenyl and substituted-phenyl, instead of the pyridine "A" ring, were equally or more active than **1a**. These include compounds **9a−b**, **9e**, **9g−h**, and **9j−u** (Table 2 and Figure S2B,C). Third, a guanidine-type connection between the "B" and "C" rings may not be required, as compound **9e** that is lacking such function was also found to be quite active (Table 2 and Figure S2C). Fourth, modification of the "C"-phenyl ring as a pyridine ring, as in compound **9l** or **9n−p**, had little effect on the activity. Fifth, substitution of "D" ring with F, CF_3, or OMe, as in compounds **1c−d** and **2j**, reduced the activity. However, there was little effect when the "D−E" ring connection was moved from the "1,4" to "1,3" position, as shown by comparing compounds **1a** versus **6a** (Schemes 1 and 2 and Table 2). Finally, compounds possessing an alkyl amine or cyclic amine instead of the piperazine (E) ring were equally as active as the parent compound. At least one amine "N" was required in the "E" ring, where the position of "N" was also important. For example, compound **1k** is active, whereas the positional isomer **1g** and compound **1j** that are lacking "N" are inactive.

2.2. 1a-Analogues, 2a−b and 3a−c Inhibited Production of Aβ Peptide in N2a695 Cells Potently and Accumulated in Mouse Brain. We focused on five hit compounds, **2a−b** and **3a−c**, and examined their effects on both Aβ40 and Aβ42 levels at 2.5−10 μM concentrations. All compounds reduced both Aβ40 and Aβ42 significantly in N2a695 cells at 5 and 10 μM concentrations, with an apparent IC50 less than 10 μM and greater than 5 μM. All five compounds have shown cell viability comparable to the DMSO control confirming that the effect on Aβ levels was not due to toxicity (Figure 2B).

We determined the brain permeability and retention of compounds **2a−b** and **3a−c**, as compared to **1a**, in 8 weeks old C57BL/6J male mice by administering compounds i.p. (50−150 mg/kg), collecting both mouse brain and plasma 4 h post injection, and extracting with ethanol or acetonitrile as described (see: General Methods). **1a** is known to not accumulate efficiently in brain because of rapid efflux by the BBB,[28] and this is reflected in the low brain concentrations of **1a** detected 4 h post administration (Figure 2C). In contrast, the new tested analogues accumulated in the brain at relatively high concentrations (between 21 and 127 pg/g, when administered at a dose of 50 mg/kg) and were found in plasma at higher concentrations (1.0−11.6 μM).

2.3. 1a and Its Analogues Reduce Aβ Production in a Similar Manner. Next, we determined whether **1a**-analogues lower Aβ levels by affecting β-cleavage of APP similarly to **1a**. For this, we performed western blotting (WB) experiments with the cell lysates obtained from the compound treatments

DOI: 10.1021/acs.jmedchem.8b02007
J. Med. Chem. XXXX, XXX, XXX−XXX

Table 2. Structure of 1a-Analogues: Series 8 Possessing Modified DE Rings, and Series 9 Possessing One or More of ABC Rings Different from 1a with/without Modification in the E Ring

ID	Structure	ID	Structure	ID	Structure
8a	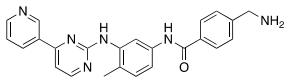	8b	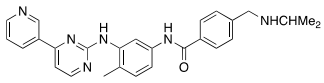	8c	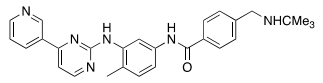
8d	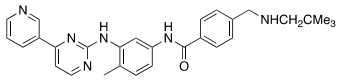	8e	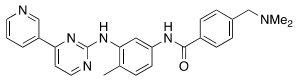	8f	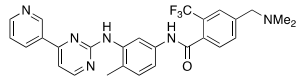
8g	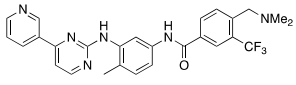	8h	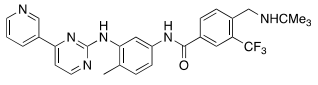	8i	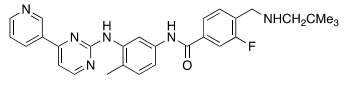
8j	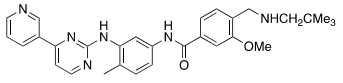	8k	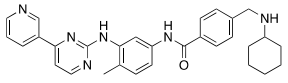	8l	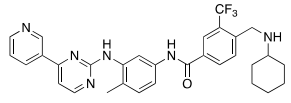
8m	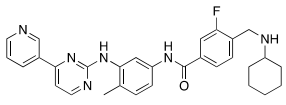	8n	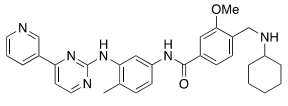	8o	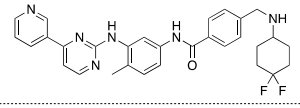
8p	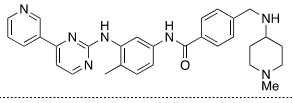	8q	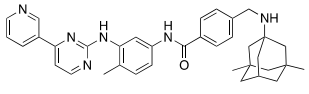	9b	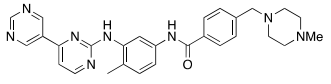
9c	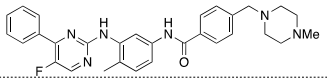	9d	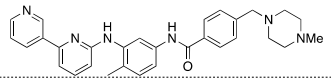	9e	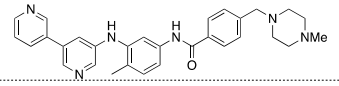
9f	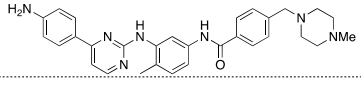	9g	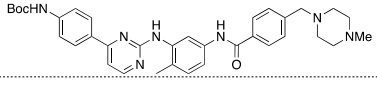	9h	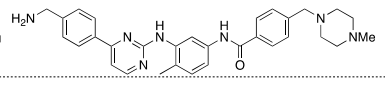
9i	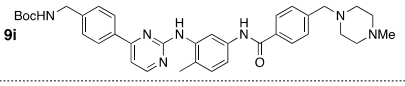	9j	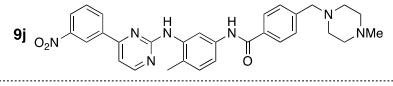	9k	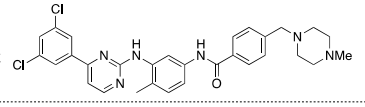
9l	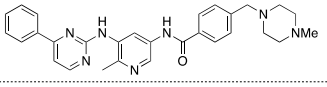	9m	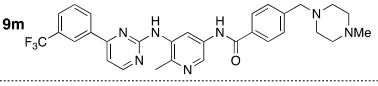	9n	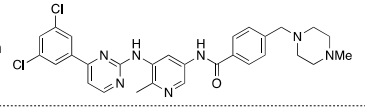
9o	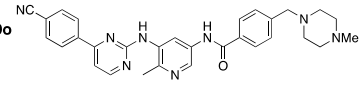	9p	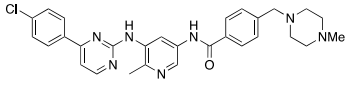	9q	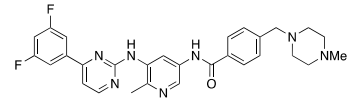
9s	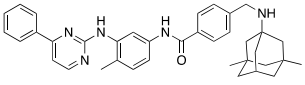	9t	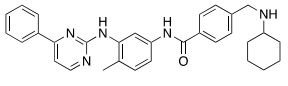	9u	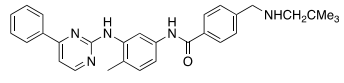

and probed the blots using antibody RU369 that recognizes APP-CTFs.[29] As shown in Figure 3A,B, cell lysates from **1a** and all its analog-treated samples reveal intense bands for APP CTFs compared to those from the control DMSO-treated samples. In addition, there are multiple APP CTFs, including 16 kDa CTF-141, comprising 141 amino acid residues and the 10 kDa CTF (weak band), in cell lysates from **1a** and all its analogues tested. It should be noted that the 10 kDa-CTF migrating near βCTF is not a product of BACE cleavage, and that the CTF-141 and other long APP CTFs in **1a**-treated samples fractionate with the lysosome.[14] Compounds **2a** and **3a** produced significantly higher levels of the 16 kDa CTF-141 than compounds **1a**, **2b**, **3b**, or **3c**, as observed in WB experiments (Figure 3A,B). Interestingly, a 16 kDa CTF is also produced from cells transfected with the APP A673T mutant.[14] The latter is a protective mutation found in Icelandic populations.[30] However, the significance of 16 kDa CTF-141 from APP-WT or with AD mutations remains to be understood.

Next, we examined the effects of **1a**-analogues on β- and γ-cleavages of APP by transfecting N2a cells with plasmids expressing FL APP695 (APP-FL) and β-CTF (APP-C99) and incubating with analogues **2a**, **2b**, **3a**, and **3c**. For a comparison, we also used a BACEi (BACE IV) or a GSi (DAPT) and determined both Aβ40 and Aβ42 peptides as well as sAPPα and sAPPβ by measuring them using MSD ELISA. The results are shown in Figures 3C,D and S3A. As expected, BACE IV and DAPT reduced the Aβ levels in cells expressing APP-FL, and DAPT also reduced Aβ in cells expressing APP-C99 (Figure 3C). Compound **1a** and its analogues also reduced the Aβ levels in cells transfected with APP-FL, but not as much in cells transfected with APP-C99. However, there is a

DOI: 10.1021/acs.jmedchem.8b02007
J. Med. Chem. XXXX, XXX, XXX−XXX

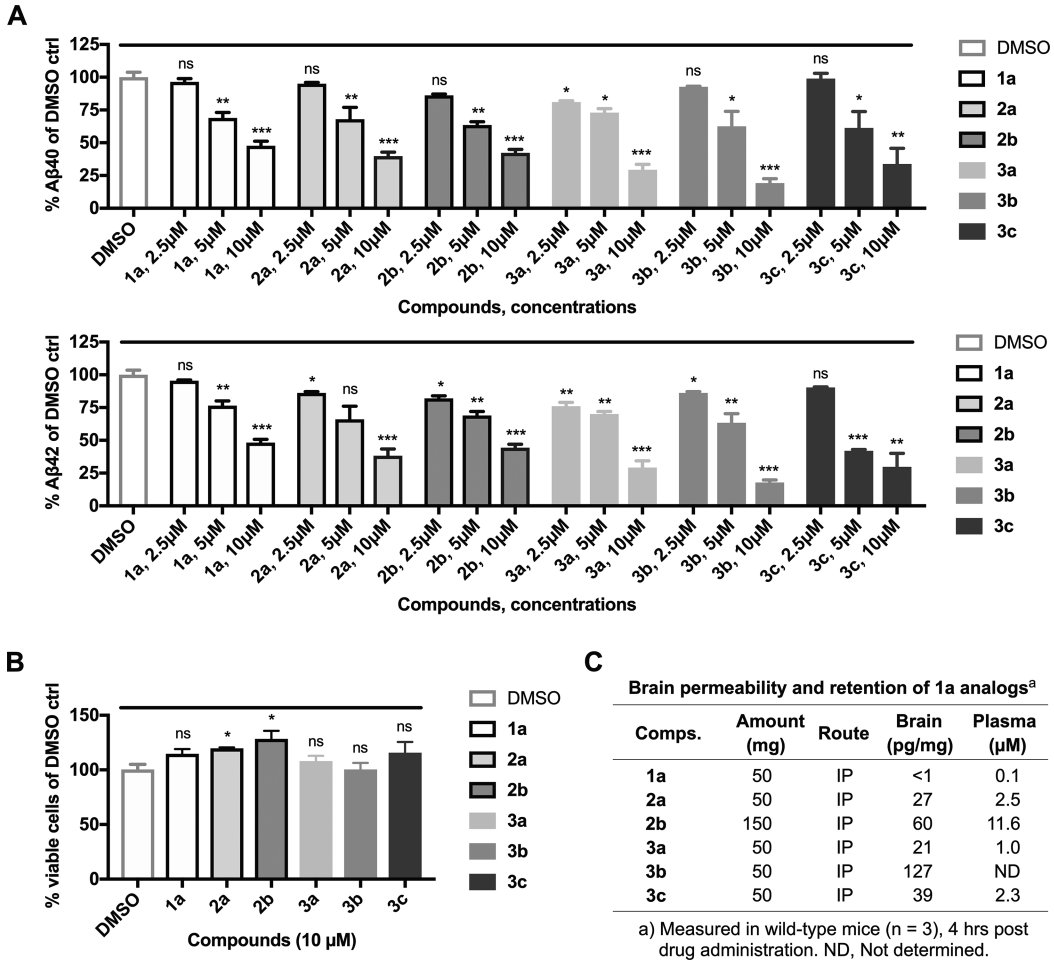

Figure 2. In vitro and in vivo evaluations of **1a**-analogues. (A) Compounds **2a**−**b** and **3a**−**c** reduced production of Aβ40 and Aβ42 peptides in N2a695 cells with an apparent IC50 between 10 and 5μM. DMSO and **1a** were used as the negative and positive controls, respectively. Results presented in (A) are the average of two or three experiments. (B) Compounds **1a** and **3a**−**3c** are nontoxic to N2a cells at 10 μM concentration, whereas **2a**−**2b** slightly increased cell density in the 5 h assay. (C) Brain and serum concentration of **1a**-analogues as determined in brain and serum extracts (n = 3 or 4) using liquid chromatography (LC)−mass spectrometry (MS)/MS. Statistical significance (P): *, <0.05%; **, <0.01%; and ***, <0.001%.

clear trend of Aβ reduction in the latter case also, where compounds **2b** had shown a ∼25% reduction of Aβ40 or of both Aβ40 and Aβ42 in APP-C99—transfected cells. Because neither **1a** nor its five analogues affected BACE1 activity, in vitro, at 10 μM concentration (Figure S3B), the reduced β-cleavage of APP could be due to an increase in alternative cleavages of APP that produce larger CTFs, including CTF-141 or could be the result of increased trafficking of APP to lysosomes, thereby reducing APP exposure to secretases.[14] Production of the large CTFs might also account for the observed reduction of both sAPPβ (by 40−75%) and sAPPα (by 20−45%) levels (Figure 3D). An increase in APP αCTF levels in **1a** and analogue-treated samples suggests that the larger CTFs preferentially undergo α-cleavage, possibly because of a reduction in the competing BACE cleavage. An increase in the APP level (with compound **3c**) could be due to a decrease in APP metabolism.

We selected compound **2a** to carry out a pilot in vivo study for several reasons. First, compounds **2a** and **3a** had shown that they produced the 16 kDa CTF-141 significantly higher than **1a** and the other three compounds, **2b** and **3b**−**c**. Second, both compounds **2a** and **3a** accumulated in mouse brain in similar quantity, but the former had a significantly higher serum concentration than the latter. Third, when we fed WT mice with an increasing amount, up to 150 mg of compound **2a** orally (gavage) for five days, we did not notice any toxicity. In fact, all mice appeared more active. Additionally, we were able to design and achieve a multigram synthesis of compound **2a** using relatively cheap starting materials without any chromatographic separation.

2.4. Compound 2a Possessed Metabolic Stability Comparable to the Parent Compound, 1a. We determined and compared the metabolic stabilities of **1a** and **2a** by adding these to mouse or human liver microsomes and measuring the remaining unmodified **1a** and **2a** in reaction mixtures.[31] In brief, **1a** and **2a** were incubated at two different concentrations, 1 and 10 μM, with either mouse or human liver microsomes, and the remaining amounts of **1a** and **2a** were determined after 30 and 60 min by high-pressure liquid chromatography (HPLC)−MS/MS analysis.[32] The results shown in Figure 4A corroborated the prior report that compound **1a** metabolizes more readily in mice than in humans.[33] We have now found that compound **2a** also metabolizes more readily in mice than in humans. Moreover, both compounds **1a** and **2a** possess comparable metabolic

DOI: 10.1021/acs.jmedchem.8b02007
J. Med. Chem. XXXX, XXX, XXX−XXX

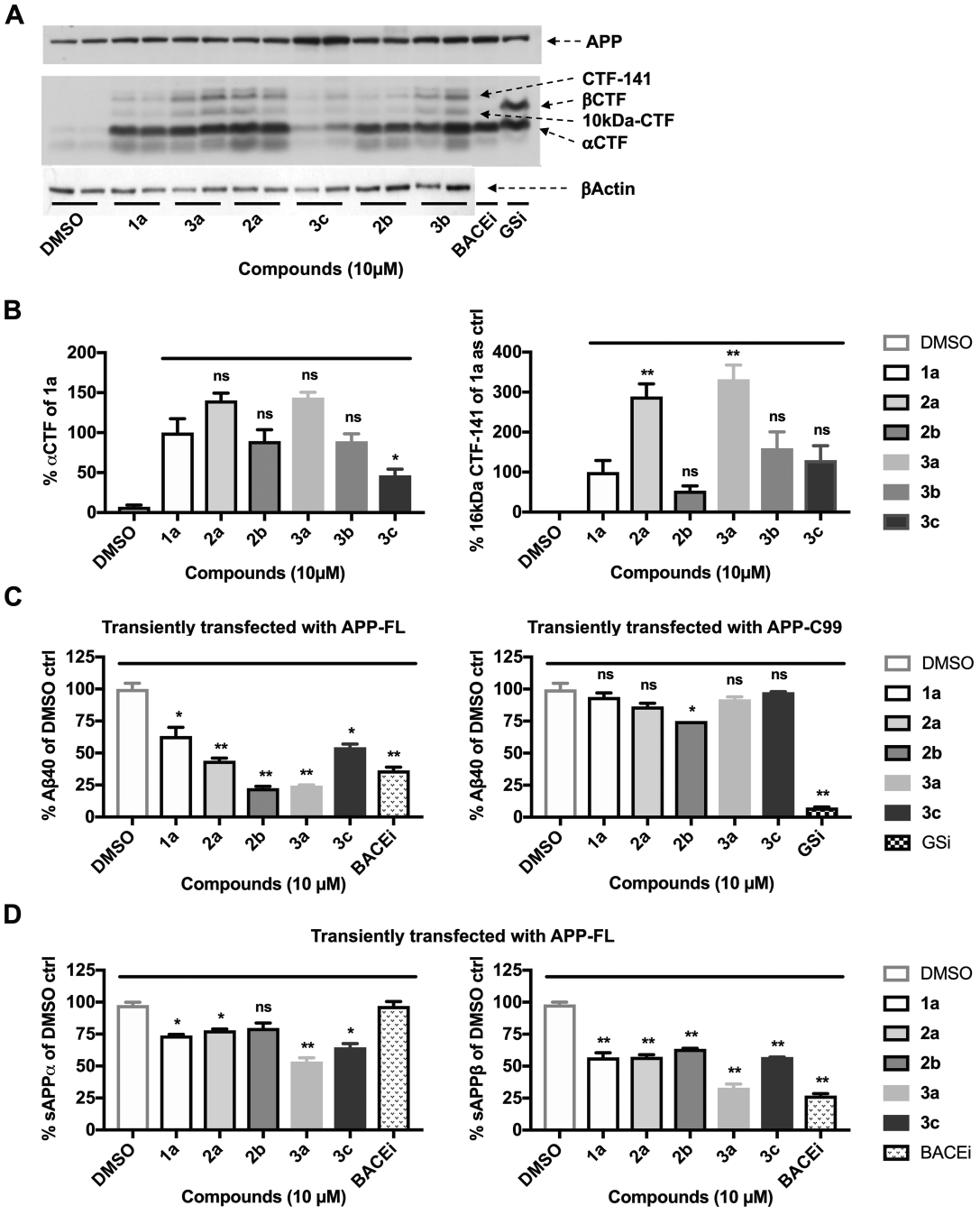

Figure 3. Effects of **1a**-analogues on APP metabolism modeled in N2a695 cells and in N2a cells transiently expressing human APP full length (APP-FL) or APP-C99. Shown are: WB analysis of N2a695 cell lysates post compound treatment shows formation of the 16 kDa (CTF-141) and 10 kDa CTF and αCTF in [(A) the labels are not in chronological order] and quantification of CTF-141 and the 10 kDa CTF bands produced in (B). Note that the 10 kDa CTF band runs just below the βCTF (12 kDa). Shown in (C and D) are: Aβ40, sAPPα, and sAPPβ levels in media from cells, transfected with plasmids for APP-FL or APP-C99 and treated with **1a** or its analogues (10 μM), BACEi (BACE IV, 2 μM), or GSi (DAPT, 1 μM). The Aβ40, Aβ42 (data shown in Figure S3A), sAPPα, and sAPPβ levels were measured using the MSD ELISA. Results presented here are the representatives of two or three independent experiments. Statistical significance (P): *, <0.05%; **, <0.01%.

stability, and compound **2a** is suitable for studies in humans, if found to effectively reduce Aβ levels in an AD mouse model.

2.5. Compound 2a Reduced Aβ Levels in 2xTg AD Mouse Brain. To determine the effects of **2a** on Aβ production/secretion, we performed a pilot study using the 2xTg AD mouse model. The latter harbors the APP Swedish and PS1ΔE9 mutations, and begins to form amyloid plaques in the brain by 6 months of age with abundant plaques present at 9 months.[34] We first determined the dosing requirements by administering **2a** to wild-type mice and measuring its accumulation in the brain and plasma over a 24 h period. Compound **2a** (50 mg/kg as a mesylate salt solution in water containing 0.1% methylcellulose) was administered by gavage, and its concentration measured in the brain and plasma extracts, as described previously using LC−MS/MS, 2, 4, 8, 12, and 24 h post gavage. As shown in Figure S4, **2a** was detected in nearly steady amounts during the first 6 h in the brain and 12 h in plasma, but it was completely washed out at the 24-h

DOI: 10.1021/acs.jmedchem.8b02007
J. Med. Chem. XXXX, XXX, XXX−XXX

A

Stability of 2a in liver microsomes

	Mouse				Human			
	1a (%)[a]		**2a** (%)[a]		**1a** (%)[a]		**2a** (%)[a]	
time	1μM	10μM	1μM	10μM	1μM	10μM	1μM	10μM
0.5 h	7.3	22.5	7.9	15.1	40.4	95.4	61.9	77.1
1.0 h	1.7	5.1	1.3	2.3	15.9	66.4	29.2	56.5

a) % Unmodified compounds, n= 3.

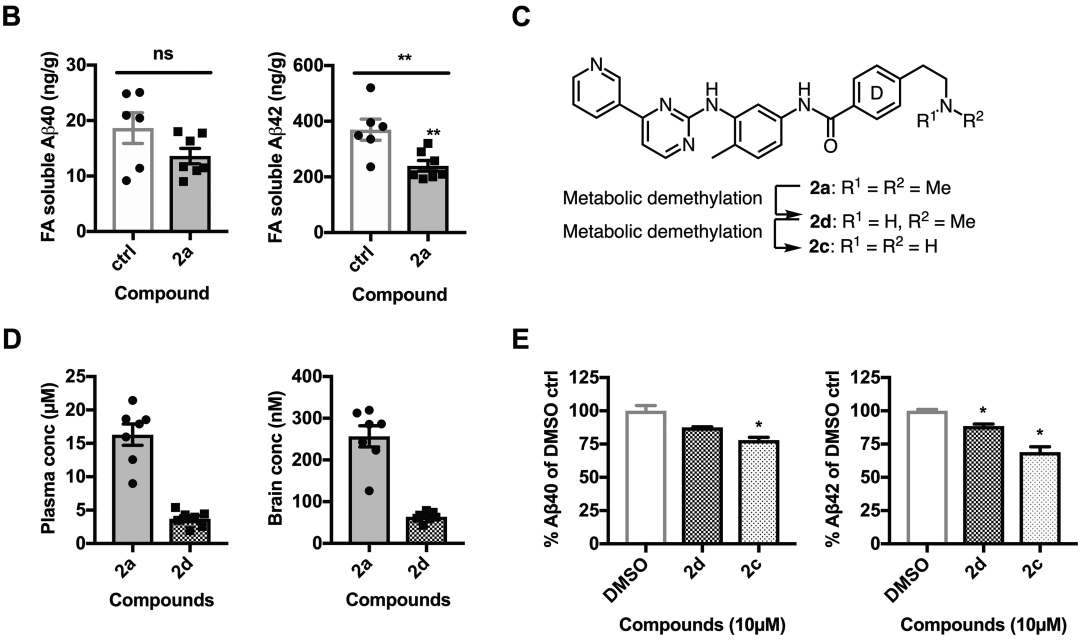

Figure 4. In vitro and in vivo evaluation of compound **2a**. (A) Microsomal stability of **1a** and its analog **2a**, measured by incubating these compounds with mouse and human liver microsomes, and determining the remaining compounds periodically using LC−MS/MS. (B) Analog **2a** reduced Aβ40 and 42 levels in 2xTg AD mice. Effects of **2a** on insoluble Aβ40/42 were determined in 5-month old 2xTg AD mice (n = 6 or 7). (C) Metabolic demethylation of **2a** affords **2c** via **2d**. (D) Metabolite **2d** is detected in the brain and plasma extracts of AD mice by performing LC−MS/MS analysis at the end of the 5-day in vivo study, and (E) compounds **2c** and **2d** reduce Aβ40 and/or Aβ42 weakly in N2a695 cells. Statistical significance (P): *, <0.05%; **, <0.01%.

time point. Because compound **2a** had shown no toxicity when it was administered orally (gavage), 150 mg/kg once a day for 5 days, we chose to administer **2a**-mesylate as aqueous solution to AD female mice (n = 7) at an elevated dose, 100 mg/kg twice daily with at least 8 h between the two administrations for 4 days and once on day 5. We obtained TBS-soluble and formic acid (FA)-soluble Aβ by performing extraction of brain tissue using 1% Triton-x100 TBS buffer (pH 7.4) and 70% FA, respectively, as described,[35] and determined the Aβ levels using ELISA. We found that TBS-soluble Aβ levels were too low to measure without large errors. In contrast, there were sufficient amounts of FA-soluble Aβ40 and Aβ42, which could be measured with great accuracy. As shown in Figure 4B, there were large reductions in both Aβ40 and Aβ42 levels in the drug-treated mice compared to the control mice, but only Aβ42 was significantly reduced (p < 0.01).

We anticipated that compound **2a** could undergo metabolic oxidative demethylation and didemethylation to produce demethylated and didemethylated products, **2d** and **2c** (Figure 4C), similarly to **1a** that affords demethylated-**1a** besides other metabolites.[36] Therefore, we performed LC−MS/MS analysis of the extracts of brain homogenates and plasma samples from **2a**-treated AD mice to determine the levels of both **2a** and the potential metabolites, **2d** and **2c**. As shown in Figure 4D, we found that approximately 15−20% of the drug in both brain and plasma consisted of metabolite **2d**. We did not examine the amounts of **2c** in these samples. To examine whether these metabolites retain Aβ-lowering activity, we prepared these compounds and evaluated them at 10 μM concentration in N2a695 cells. Indeed, both metabolites, **2d** and **2c**, reduced the levels of secreted Aβ42 peptide significantly (p < 0.05), whereas compound **2c** also reduced the levels of Aβ40 peptide (Figure 4E). Thus, the observed activity of compound **2a** in AD mouse model, in vivo, could still be the combined effects of all three compounds, that is, the parent drug, **2a**, and its metabolites, **2c−d**.

2.6. Perspective. Accumulation of two key neurotoxic agents, Aβ peptides and hyperphosphorylated tau (pTau) protein, in an AD brain starts decades ahead of when the actual sign of the disease becomes evident and is followed by neuronal loss and dementia.[37] Although aging is a major causative factor of AD,[38] the Aβ peptides and pTau protein levels increase with age both in AD patients and in non-AD people.[39−41] It can be argued that reducing the production of Aβ peptides and pTau protein starting early on in life could improve cognition and dementia of both AD patients and of non-AD individuals. Earlier, compound **1a** has been shown to prevent Abl-dependent tau phosphorylation[42] and Aβ fibrils-induced apoptosis in rat models.[43] We anticipate that the **1a**-analogues, **2a−b** and **3a−c**, which inhibit Abl kinase potently

DOI: 10.1021/acs.jmedchem.8b02007
J. Med. Chem. XXXX, XXX, XXX−XXX

A

% Inhibition of Abl kinase

Comp	Conc (μM)	Abl1 (%)
1a	10	99
	3.3	98
	1.0	95
2a	10	88
	5.0	81
	2.5	68
2b	10	96
	5.0	93
	2.5	90
3a	10	73
	5.0	57
	2.5	42
3b	10	86
	5.0	79
	2.5	70
3c	10	92
	5.0	88
	2.5	79

B

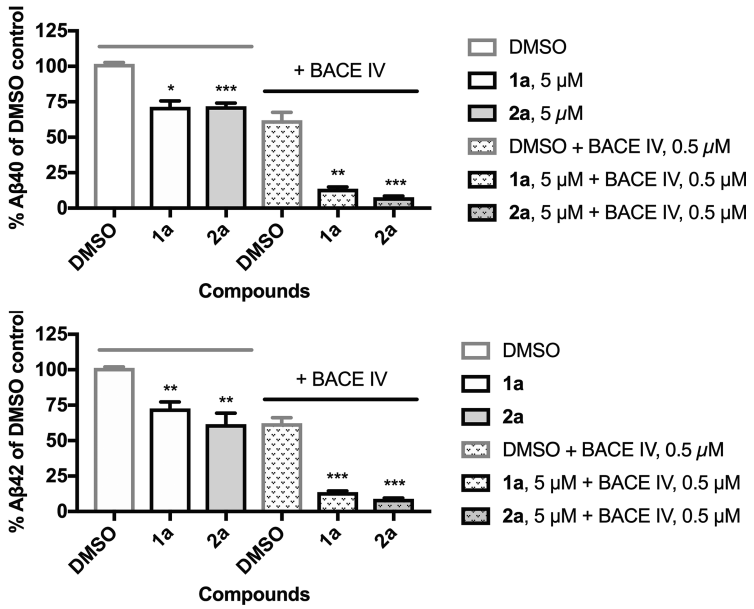

Figure 5. Effects of (A) **1a**-analogues on Abl kinase inhibition (performed by an outsourced company: Luceome Biotechnologies, Tucson, AZ), and (B) **2a** on Aβ40 and Aβ42 production in combination with BACE IV and Abl and ic-Kit kinase inhibition. N2a695 cells were pretreated with BACE IV for 1 h before treatment with **1a** or **2a** (and BACE IV) for 5 h. Aβ40 and Aβ42 levels were measured using commercially available ELISA kits for human Aβ40 and Aβ42. Statistical significance (*P*): *, <0.05%; **, <0.01%, ***, <0.001%.

(Figure 5A), could also reduce Abl-dependent tau phosphorylation. Separately, Netzer, et al., have shown that **1a** reduces production of Aβ peptides independent of Abl kinase inhibition.[13] By analogy, we argue that compounds **2a**–**b** and **3a**–**c** could also be inhibiting production of Aβ peptides independent of Abl kinase inhibition. Nevertheless, a direct measurement of these compounds and any future **1a**-analogues in Abl knockout cells may be desirable to confirm that the effects of **1a**-analogues on Aβ production are indeed Abl independent.

Another key feature of **1a** is that it can be combined with a BACEi to reduce production of Aβ peptides by lessening the BACEi-related toxicity. BACE1 inhibition is considered a highly desirable strategy for treating or preventing AD, which is evident from the fact that multiple clinical trials with small molecule BACEi's are in progress.[44] However, no BACEi has yet been successful in clinical trials, as BACE1 has many cellular substrates and by inhibiting processing of all or most of these substrates, nonselective BACE1 inhibitors cause serious side effects.[45] We have previously shown that a combination of **1a** and a BACEi, BACE IV, reduces Aβ levels in N2a695 cells in a synergistic manner.[14] We have now found that a combination of compound **2a** with BACE IV caused greater reduction in the production of the Aβ peptide, than using compound **2a** alone, similarly to the **1a**-BACE IV combination.[14] We will continue screening **1a**-analog/BACEi combinations in our future studies to identify those that mediate synergistic effects at low BACEi concentration.

3. CONCLUSIONS

In this study, we have developed chemical analogues of **1a** that possess comparable activities. The new analogues also function similarly to the parent compound and reduce Aβ levels in N2a695 cells primarily through reducing the β-cleavage of APP and shifting APP metabolism toward a nonamyloidogenic pathway. By performing an in vivo study in 5 months old 2xTg female AD mice, compound **2a** was found to have significantly reduced brain Aβ42 levels, when given at 100 mg/kg twice daily for 4.5 days. The observed effect of compound **2a** on Aβ production could indeed be the effect of both the parent drug, **2a**, and its metabolites, **2c** and **2d**. This in vivo study provides a basis to further examine compound **2a** or other analogues in larger studies for treating AD and for studies for prevention. The second, a combination therapy using compound **2a** and a BACEi could provide maximum therapeutic benefit, while reducing the effective dose of both BACEi and **2a** (or its analogues). This approach would require a potent brain-permeable BACEi. Future development of **1a**-analogues will avoid functionalities known to possess pGP activity, and include assays to determine pGP activity of such compounds and Aβ levels in Abl knock-out cells.

4. EXPERIMENTAL SECTION

4.1. General Methods. All commercial chemicals and solvents were reagent grade and used without further purification. All air-sensitive reactions were performed under argon protection. Microwave reactions were performed on a Biotage Initiator. Column chromatography was performed using CombiFlash or Biotage instruments and silica gel SNAP columns. Analytical thin layer chromatography was performed on Merck 250 μM silica gel F_{254} plates, and preparative thin layer chromatography (PTLC) on Merck 1000 μM silica gel F_{254} plates obtained from EMD Millipore corporation. Purity of final compounds was checked using Agilent 1260 Infinity Series II preparative HPLC equipped with a 1260 Infinity II Multiple wavelength detector and Gemini 5 μm C18 110 Å LC column (100 × 4.6 mm), mobile phase: acetonitrile and water (0.1% TFA), 80:20 isocratic. All final compounds were found ≥95% pure. The identity of each product was determined using MS (MS: Thermo Scientific LTQ XL; LC: Thermo Scientific Dionex UltiMate 3000) and NMR (Bruker 400 or 600 MHz instrument) using $CDCl_3$ as the solvent unless otherwise mentioned. Chemical shifts are reported in δ values in ppm downfield from TMS as the internal standard. ^{1}H data are reported as follows: chemical shift, multiplicity

DOI: 10.1021/acs.jmedchem.8b02007
J. Med. Chem. XXXX, XXX, XXX−XXX

(s = singlet, d = doublet, t = triplet, q = quartet, br = broad, m = multiplet), coupling constant (Hz), integration.

4.2. Synthesis and Characterization of Compounds. *4.2.1. 4-(2-(Dimethylamino)ethyl)-N-(4-methyl-3-((4-(pyridin-3-yl)-pyrimidin-2-yl)amino)phenyl)-benzamide,* ***2a****.* DIEA (3.5 mL, 20 mmol) was added to a mixture of amine **4** (2.77 g, 10 mmol), acid **10a** (1.85 g, 10 mmol), and HATU (4.94 g, 13 mmol) in anhydrous dimethylformamide (DMF, 25 mL), and the mixture was stirred overnight at room temperature (RT). The reaction mixture was diluted with water, and the resulting solid **11a** was collected by filtration (3.15 g, 70%). A mixture of crude **11a** and Me_2NH (30 mL, 40% in water) in a pressure bottle was heated at 120 °C overnight. The reaction mixture was cooled and filtered, and the resulting white solid was washed with water. The solid was dissolved in MeOH, coevaporated with toluene, and triturated with MeOH to afford **2a** (2.60 g 59% yield) upon filtration. ^{1}H NMR (600 MHz) of **2a**: δ 9.27 (s, 1H), 8.73 (d, J = 3.6 Hz, 1H), 8.61 (s, 1H), 8.55 (d, J = 4.2 Hz, 2H), 7.84 (d, J = 6.0 Hz, 2H), 7.45 (t, J = 6.60 Hz, 1H), 7.35 (d, J = 7.80 Hz, 2H), 7.32 (d, J = 7.80 Hz, 1H), 7.24−7.21 (m, 2H), 7.05 (s, 1H), 2.90 (t, J = 7.80 Hz, 2H), 2.62 (t, J = 7.80 Hz, 2H), 2.38 (s, 3H), and 2.36 (s, 6H). ^{13}C NMR (150 MHz, DMSO-d_6): δ 165.78, 162.07, 161.66, 159.94, 151.85, 148.67, 144.92, 138.26, 137.72, 134.89, 133.17, 132.69, 130.48, 129.04, 128.04, 124.25, 117.66, 117.18, 107.97, 60.88, 45.22, 33.56, and 18.11. HRMS (ESI), m/z: 453.2398 [M + H]$^+$. Purity (HPLC): >98%.

4.2.2. 4-(2-(Dimethylamino)ethyl)-N-(4-methyl-3-((4-(pyridin-3-yl)pyrimidin-2-yl)amino)phenyl)-2-(trifluoromethyl)benzamide, ***2b****.* Acid **10b** (1.10, 4.0 mmol) was coupled to **4** (1.10, mmol) similarly as described above for **11a**, using HATU (1.82 g, 4.8 mmol) and iPr$_2$EtN (1.5 mL, 8 mmol) in DMF (12 mL) to afford intermediate **12a** (1.6 g, 75%). ^{1}H NMR (600 MHz) of **12a**: δ 9.19, (s, 1H), 8.65 (d, J = 6.0 Hz, 1H), 8.50 (d, J = 6.0 Hz, 1H), 8.49 (d, J = 6.0 Hz, 1H), 8.44 (s, 1H), 7.88 (s, 1H), 7.78 (d, J = 6.0 Hz, 1H), 7.54 (d, J = 12.0 Hz, 1H), 7.44 (dd, J = 6.0, 6.0 Hz, 1H), 7.30 (d, J = 6.0 Hz, 1H), 7.22 (d, J = 12.0 Hz, 1H), 7.19 (d, J = 6.0 Hz, 1H), and 2.35 (s, 3H). MS, m/z: 528.0 [M + H]$^+$.

To a degassed mixture of intermediate **12a** (528 mg, 1.0 mmol), (E)-1-ethoxyethane-2-boronic acid pinacol ester (257 mg, 1.30 mmol), and Cs_2CO_3 2 M solution (1 mL) in 1,4-dioxane (3 mL/mmol) in a microwave vial was added $Pd(PPh_3)_4$ (55 mg, 5 mol %). After the reaction mixture was heated at 100 °C for 45 min using a microwave, it was diluted with water and extracted with CH_2Cl_2. The organic layer was adsorbed over silica gel and chromatographed affording the ethoxyvinyl-coupled product, **13a** (450 mg, 85%). MS: m/z 520.4 [M + H]$^+$.

TFA (1.0 mL) in DCM (20 mL) was added to the above-described intermediate, and the mixture was stirred overnight at RT. Volatile materials were removed under reduced pressure, and the resulting aldehyde was taken to next step without further purification. MS: m/z 492.3 [M + H]$^+$.

Me_2NH (10 mL, 4 M in THF) was added to a solution of the above-described aldehyde intermediate in CH_2Cl_2 (10 mL) in a pressure bottle. After the mixture was stirred for 1 h at RT, it was cooled and $NaCNBH_3$ (130 mg, 2 mmol) was added, and stirring was continued overnight. Solvents were removed, and the residues were suspended in CH_2Cl_2 and washed with brine. Combined organic layers were dried over anhydrous $MgSO_4$, inorganic materials were separated by filtration, organic layers were concentrated under reduced pressure, and the residue was chromatographed over SiO_2 gel using CH_2Cl_2−MeOH−aq NH_3 to afford compound **2b** (235 mg, 45% based on **13a**). ^{1}H NMR (600 MHz, CD_3OD) of **2b**: δ 9.13 (s, 1H), 8.60 (d, J = 3.3 Hz, 1H), 8.53 (d, J = 7.9 Hz, 1H), 8.45 (d, J = 2.0 Hz, 2H), 8.37 (s, 1H), 7.59 (s, 1H), 7.56 (d, J = 7.8 Hz, 1H), 7.53 (d, J = 7.6 Hz, 1H), 7.46 (dd, J = 7.8, 4.9 Hz, 1H), 7.35 (s, 1H), 7.26 (d, J = 7.8 Hz, 1H), 7.19 (d, J = 8.2 Hz, 1H), 7.18 (d, J = 5.2 Hz, 1H), 3.00 (br s, 4H), 2.62 (s, 6H), and 2.31 (s, 3H). ^{13}C NMR (150 MHz, DMSO-d_6): δ 165.99, 162.03, 161.58, 159.97, 151.85, 148.65, 143.43, 138.36, 137.47, 134.88, 134.55, 133.07, 132.71, 130.62, 128.25, 126.79, 126.31, 125.24, 124.20, 123.42, 116.89, 116.45, 60.41, 45.40, 32.86, and 18.13. HRMS (ESI), m/z: 521.2264 [M + H]$^+$. Purity (HPLC): >98%.

4.2.3. N-(4-Methyl-3-((4-(pyridin-3-yl)pyrimidin-2-yl)amino)-phenyl)-4-(4-methylpiperazin-1-yl)benzamide, ***3a****.* Amine **4** (1.39, 5.0 mmol) was coupled with acid **10c** (1.10 g, 5.0 mmol) similarly as described above for **11a**, using HATU (2.25 g, 6.0 mmol) in anhydrous DMF (mL) and iPr$_2$EtN (1.75 mL, 10 mmol) at 60 °C (2 h) than at RT overnight to afford **3a** (1.20 g, 50%) after the usual work-up and chromatographic separation using CombiFlash (CH_2Cl_2−MeOH, 15%). ^{1}H NMR (400 MHz) of **3a**: δ 9.19 (br s, 1H), 8.64 (d, J = 4.0 Hz, 1H), 8.50−8.46 (m, 2H), 8.42 (br s, 1H), 7.79 (t, J = 8.0 Hz, 3H), 7.62 (d, J = 8.0 Hz, 1H), 7.42 (t, J = 8.0 Hz, 1H), 7.31 (m, 1H), 7.17 (dd, J = 8.0, 4.0 Hz, 2H), 6.90 (d, J = 8.0 Hz, 1H), 3.39 (br s, 4H), 2.80 (br s, 4H), and 2.49 and 2.32 (s, 3H each). ^{13}C NMR (150 MHz, DMSO-d_6): δ 165.30, 162.06, 161.70, 159.93, 153.43, 151.84, 148.66, 138.18, 138.02, 134.89, 132.70, 130.39, 129.47, 129.47, 127.64, 124.24, 117.67, 117.17, 113.96, 107.91, 54.82, 47.40, 46.18, and 18.09. HRMS (ESI), m/z: 480.2496 [M + H]$^+$. Purity (HPLC): 96%.

4.2.4. N-(4-Methyl-3-((4-(pyridin-3-yl)pyrimidin-2-yl)amino)-phenyl)-4-(1-methylpiperidin-4-yl)benzamide, ***3b****.* Amine **4** (277 mg, 1.0 mmol) was coupled with acid **10e** (220 mg, 1.0 mmol) using HATU (494 mg, 1.3 mmol) and DIEA (0.350 mL, 1.3 mmol) in anhydrous DMF (3.0 mL) as described above for **11a** to afford **3b** (200 mg, 42%). ^{1}H NMR (600 MHz, DMSO-d_6) of **3b**: δ 10.10 (s, 1H), 9.25 (s, 1H), 8.94 (s, 1H), 8.66 (d, J = 6.0 Hz, 1H), 8.48 (d, J = 6.0 Hz, 1H), 8.45 (d, J = 6.0 Hz, 1H), 8.05 (s, 1H), 7.86 (d, J = 6.0 Hz, 1H), 7.50 (td, J = 6.0 Hz, 1H), 7.46 (d, J = 6.0 Hz, 1H), 7.40 (d, J = 6.0 Hz, 1H), 7.37 (d, J = 6.0 Hz, 1H), 7.18 (d, J = 12.0 Hz, 1H), 2.91 (br, 2H), 2.55 (m, 1H), 2.23 and 2.20 (s, 3H each), 2.04 (br, 2H), and 1.76−1.68 (m, 4H). ^{13}C NMR (150 MHz, DMSO-d_6): δ 165.75, 162.07, 161.66, 159.94, 151.85, 150.23, 148.67, 138.26, 137.72, 134.89, 133.48, 132.69, 130.48, 124.24, 128.02, 127.17, 124.25, 117.64, 167.15, 107.98, 55.97, 46.33, 41.25, 32.97, and 18.11. HRMS (ESI), m/z: 479.2550 [M + H]$^+$. Purity (HPLC): >98%.

4.2.5. N-(4-Methyl-3-((4-(pyridin-3-yl)pyrimidin-2-yl)amino)-phenyl)-4-(1-methylpiperidin-3-yl)benzamide, ***3c****.* Amine **4** (106.0 mg, 0.382 mmol) was coupled with acid **10g** (128.0 mg, 0.42 mmol) using HATU (172.0 mg, 0.42 mmol) and DIEA (0.097 mL, 0.76 mmol) in anhydrous DMF (3.0 mL) as described above for **11a** to afford the Boc-protected precursor (80 mg, 37%) of **3f**. The latter was deprotected using 4 M HCl in dioxane (0.500 mL) as above to afford **3f** (50 mg, 60%) as a HCl salt. ^{1}H NMR (400 MHz, CD_3OD) of **3f**: δ 9.26 (s, 1H), 8.61 (d, J = 3.7 Hz, 1H), 8.57 (d, J = 7.8 Hz, 1H), 8.45 (d, J = 4.9 Hz, 1H), 8.22 (s, 1H), 7.90 (d, J = 7.8 Hz, 2H), 7.52 (m, 1H), 7.39 (m, 3H), 7.33 (d, J = 5 Hz, 1H), 7.24 (d, J = 8.1 Hz, 1H), 3.18 (d, J = 10.8 Hz, 2H), 2.73−2.88 (m, 3H), 2.31 (s, 3H), 2.00 (m, 1H), 1.89 (m, 1H), and 1.73 (m, 2H). MS: m/z 465.3 [M + H]$^+$. Purity (HPLC): >98%.

Amine **3f** (40 mg, 0.107 mmol) was methylated using paraformaldehyde (10 mg, 0.300 mmol) and $NaCNBH_3$ (20 mg, 0.30 mmol) in CH_2Cl_2 (3 mL) in a tightly-capped bottle to afford **3c** (10 mg, 20%) after the usual work-up and silica gel PTLC using CH_2Cl_2−MeOH−aq NH_3 as the mobile phase. ^{1}H NMR (600 MHz, DMSO-d_6) of **3c**: δ 10.18 (s, 1H), 9.28 (s, 1H), 8.98 (s, 1H), 8.68 (dd, J = 4.8, 1.2 Hz, 1H), 8.52 (d, J = 5.4 Hz, 1H), 8.48 (d, J = 8.4 Hz, 1H), 8.08 (s, 1H), 7.96 (d, J = 8.4 Hz, 2H), 7.52 (m, 1H), 7.48 (dd, J = 7.8, 1.2 Hz, 1H), 7.44 (m, 1H), 7.22 (d, J = 8.4 Hz, 1H), 3.50 (d, J = 10.8 Hz, 1H), 3.45 (d, J = 11.4 Hz, 1H), 3.14 (t, J = 11.4 Hz, 1H), 3.06 (m, 1H), 2.95 (m, 1H), 2.81 (s, 1H), 2.23 (s, 3H), 1.97 (d, J = 12.0 Hz, 1H), 1.92 (d, J = 12.0 Hz, 1H), 1.80 (m, 1H), and 1.66 (m, 1H). ^{13}C NMR (150 MHz, DMSO-d_6): δ 165.42, 162.07, 161.65, 159.96, 151.84, 148.67, 145.14, 138.29, 137.56, 134.89, 134.45, 132.68, 130.53, 128.55, 128.17, 127.57, 124.25, 117.70, 117.22, 108.11, 57.92, 53.70, 43.52, 29.07, 23.01, and 18.12. HRMS (ESI), m/z: 479.2547 [M + H$^+$]. Purity (HPLC): >98%.

4.3. Evaluation of Compounds in Cells. *4.3.1. Screening and Evaluation of* ***1a****-Analogues.* N2a695 cells were used to screen all **1a**-analogues and in the follow-up studies with compounds found active in the preliminary screen. Cells were cultured in 1:1 Opti-MEM

DOI: 10.1021/acs.jmedchem.8b02007
J. Med. Chem. XXXX, XXX, XXX−XXX

Reduced Serum Media (Life Technologies): Dulbecco's modified Eagle medium ([+] 4.5 g/L D-glucose; [+] L-glutamine; [-] sodium pyruvate (Life Technologies) supplemented with 5% fetal bovine serum, 0.4% penstrep, and 0.4% geneticin and incubated at 37 °C in 5% CO_2.

In a typical experiment, 6-well tissue culture plates (Corning) were seeded at 4.0×10^5 to 4.5×10^5 N2a695 cells/mL, 2 mL/well for overnight incubation. Media were carefully removed and fresh media containing 10 μM solution of compounds (prepared from 10 mM solution in DMSO) were gently layered onto adherent cells (>95% confluent). Appropriate dilution of compounds was performed in DMSO before adding to media. After cells were incubated with compounds for 5 h at 37 °C in 5% CO_2, culture media were collected. To measure soluble Aβ concentrations in the culture media, these were transferred to strips of a 96-well ELISA plate for human Aβ40 peptide or to a 96-well V-PLEX Plus MSD (Mesoscale Discovery) plate for Aβ Peptide Panel 1 (6E10) Kit (Catalog number K15200G) and processed as per manufacturer instructions. Signals for Aβ were measured using a PerkinElmer EnVision and SQ120 MSD ELISA reader. Follow-up studies with N2a695 cells were performed similarly.

*4.3.2. In Vitro Metabolic Stability of **1a**-Analogues.* Compound **1a** and analogues (1 and 10 μM) were incubated with human or CD-1 mouse liver microsomes (0.5 mg protein/mL) and appropriate cofactors (2.5 mM NADPH and 3.3 mM $MgCl_2$) in 100 mM phosphate buffer, pH 7.4, at 37 °C. The incubation contained a final organic solvent concentration of 0.1% DMSO. Reactions were started with the addition of an NADPH/$MgCl_2$ mix and stopped by removing 100 μL aliquots at selected time points (0, 30, and 60 min) and mixing with 200 μL of acetonitrile. Following brief vortexing and centrifugation, an aliquot of the supernatant was transferred to a tube and further diluted 2-fold (for 1 μM, using 10% acetonitrile containing internal standards) or 20-fold (for 10 μM, using 37% acetonitrile containing internal standards). Subsequently, amounts of unmodified **1a** or analogues in the quenched reactions were determined using LC-MS/MS analysis.

*4.3.3. Effects of **1a**-Analogues on APP Metabolism.* N2a695 cells were treated with compounds for 5 h as described above, and media were aspirated out (or collected for determination of Aβ levels). Cells were scraped in cold Dulbecco's phosphate-buffered saline (PBS) buffer (1 mL) containing mini ethylenediaminetetraacetic acid-free protease inhibitor (Roche) and centrifuged for 1 min at 13 000 rpm at 4 °C to form a cell pellet. The buffer was aspirated, and the cell pellets were lysed in 3% SDS by sonication for two rounds of 20 s on a low setting. Protein concentrations were measured using the Pierce BCA Protein Assay (Thermo Fisher) Kit in accordance with the manufacturer's instructions.

To perform WBs, N2a695 cell lysates from **1a** and analogue-treated samples were run on a 16.5% Tris-Tricine gel (Criterion) and electrotransferred to PVDF membranes (EMD Millipore) overnight at 30 V. The PVDF membranes were incubated in PBS containing 0.25% glutaraldehyde (Sigma) for 30 min after electrotransference, blocked for 30 min in milk PBST, incubated with primary antibody RU369 for 1 h at RT followed by washing and incubation with an HRP-linked secondary antibody, and detected with enhanced chemiluminescence ECL reagents. WB images were analyzed using ImageJ to quantify the prominent bands.

To determine effects of the compounds on BACE1 versus GS inhibition, we used N2a cells transfected with FL APP (APP-FL) or with APP99 (APP-βCTF). After 48 h, media were removed and fresh media containing compound **1a** and analogues were added. Following 5 h of incubation, cell supernatants were collected, and analyzed using MSD-ELISA for Aβ and for sAPPα and β.

4.4. Evaluation of Compounds Using Mouse Models, in Vivo. All procedures involving animals were approved by The Rockefeller University Institutional Animal Care and Use Committee and were in accordance with the National Institutes of Health guidelines.

*4.4.1. In Vivo Brain Permeability and Retention of **1a** and Analogues.* Mesylate salts of **1a** analogues (1 or 3 mg/mL in water, 125 μL, 50 or 150 mg/kg) were administered intraperitoneally (i.p.) or through oral gavage to 8 weeks old C57BL/6J WT mice. The mice were euthanized 4 h post drug administration, and the brain hemispheres and plasma were harvested and collected in preweighted tubes and snap-frozen in liquid nitrogen. To measure brain and plasma concentrations of the specific compounds, mouse brain tissue was homogenized and extracted using ethanol, and plasma samples were extracted using acetonitrile. Concentration of the drug compounds and metabolites both in brain and in plasma was determined by LC-MS/MS analysis.

4.4.1.1. Drug Extraction from Brain. After the tubes were weighed to calculate brain weight and thawed to RT, 1 mL of EtOH (200 Proof) was added to the microcentrifuge tubes containing the harvested right brain hemispheres. The internal standard (ABG190, a synthetic analog of **1a,** 10 μL, 1 μM) was added to each tube, and samples were sonicated to homogeneity (~2 min). Tubes were shaken at 40 min at RT (1 K rpm) and centrifuged for 8 min at 13 K RPM. The supernatant (0.9 mL) was transferred to a new collection tube, and 0.5 mL EtOH was added to the pellet for a second round of extraction as described above. The supernatant (600 μL) was combined with the first collection before samples were submitted for LC−MS/MS analysis.

4.4.1.2. Drug Extraction from Blood. Acetonitrile (300 μL) was added to the collected blood samples. The internal standard (ABG190, 10 μL, 1 μM) was added to each tube, and the samples were sonicated to homogeneity (~2 min). The tubes were centrifuged at 13 K RPM for 9 min. The supernatant (300 μL) was collected and combined with 500 μL of 5 mM ammonium formate before the samples were submitted for LCMS-MS analysis.

*4.4.2. In Vivo Evaluation of Compound **2a** in 2xTg AD Mice.* Female mice expressing the human FAD mutations APP KM670/671NL (Swedish) and PSEN1 M146V were used in this study. Mice were obtained by performing in vitro fertilization, in house, and those positive for APP Swedish and PS1ΔE9 genes were identified by PCR-based genotyping. The WT C57BL/6J mice (The Jackson Laboratory; stock no. 000664) were used for generating 2xTg mouse pups from in vitro fertilization.

4.4.2.1. Evaluation. 2xTg AD female mice (n = 7 for each group) received 100−125 μL solution (based on mouse weight) via oral administration (gavage) of **2a**-mesylate (20 mg/mL in water containing 0.1% methylcellulose, 100 mg/kg/mouse) or with vehicle (water containing 0.1% methylcellulose, 100−125 μL) twice a day, 8 h apart in the morning and afternoon, for 4 days and in the morning on day 5. All mice were euthanized 4 h after the last injection. Brain hemispheres and plasma were harvested, collected in preweighted tubes, and the tubes were snap-frozen in liquid nitrogen. On the day of analysis, tubes containing the left-brain hemispheres were weighed after they were defrosted. Brain mass was submerged in 1% Triton-x100 TBS Buffer (pH 7.4) (2 mL), homogenized using a Dounce homogenizer and transferred to ultraclear centrifuge tubes (Beckman Coulter) in which they were ultracentrifuged at 40 000 RPM for 35 min (TLA. 100.3 100 K RPM rotor). Supernatants were collected to measure soluble Aβ peptides. Insoluble Aβ was extracted from the pellets with 70% FA (1 mL) and 20 μL aliquots were neutralized with 200 μL Bis−Tris buffer. Aβ 1−40 and Aβ 1−42 were measured using ELISA (Invitrogen) in accordance with the manufacturer's instructions.

4.4.3. Statistical Analysis. The data are presented as means ± SEM. The data were analyzed by Student's t-test for single comparison and one-way ANOVA for multiple comparisons, and those showing P value < 0.05 were considered significant.

4.4.4. In Vitro Kinase Activity Assay. The assay was performed by Luceome Biotechnolgies, LLC, using the general methods, as described.[46] Typically, 10 mM stock solutions of the compounds were diluted in DMSO to a concentration of 250 μM. Before initiating the assay, all test compounds were evaluated for a false positive against split-luciferase. For kinase assays, each Cfluc-Kinase was translated along with Fos-Nfluc using a cell-free system (rabbit reticulocyte lysate) at 30 °C for 90 min. An aliquot (24 μL) of this lysate containing either 1 μL of DMSO (for no-inhibitor control) or compound solution in DMSO (10 μM final concentration) was

DOI: 10.1021/acs.jmedchem.8b02007
J. Med. Chem. XXXX, XXX, XXX−XXX

incubated for 30 min at RT followed by 1 h in the presence of a kinase-specific probe. Luciferin assay reagent (80 μL) was added to each solution, and luminescence was immediately measured on a luminometer. The percent inhibition was calculated using the following equation: % inhibition = $(ALU_{control} - ALU_{sample} \times 100)/ALU_{control}$.

■ ASSOCIATED CONTENT

Supporting Information

The Supporting Information is available free of charge on the ACS Publications website at DOI: 10.1021/acs.jmedchem.8b02007.

General synthetic procedures and characterization of synthesized compounds including ^{1}H NMR spectra and MS data, truncated Gleevec analogues containing 3 or 4 rings, Gleevec analogues containing 4 or 5 rings and ABC rings identical to 1a and different from 1a, and figures showing screening data of all synthetic analogues and evaluation of selected compounds (PDF)

SMILES data for compounds **1a−l**, **2a−j**, **3a−i**, **4a−h**, **5**, **6a−g**, **7a−b**, **8a−q**, and **9a−u** (CSV)

■ AUTHOR INFORMATION

Corresponding Author

*E-mail: ssinha@rockefeller.edu. Phone: (212)327-8121.

ORCID

Subhash C. Sinha: 0000-0001-8916-5677

Notes

The authors declare no competing financial interest.

■ ACKNOWLEDGMENTS

We are thankful to Dr. Victor Bustos of the Rockefeller University for helpful discussions, and to Mondana H. Ghias for determining Aβ of some compounds in cellular assays early on. Funding support from JPB (#322 and #839 to SCS) is duly acknowledged.

■ ABBREVIATIONS

Aβ, β amyloid or amyloid β; AD, Alzheimer's disease; APP, amyloid precursor protein; Aq Me_2NH, aqueous dimethylamine; BACE1, β-secretase; BACEi, β-secretase inhibitor; BBB, blood−brain-barrier; Boc, butoxycarbonyl; βCTF, β-carboxy terminal fragment; CH_2Cl_2, dichloromethane; $(CH_2O)_n$, paraformaldehyde; Cs_2CO_3, cesium carbonate; DIEA, diisopropyethylamine; DMF, dimethylformamide; DMSO, dimethylsufoxide; ELISA, enzyme-linked immunosorbent assay; EtOAc, ethylacetate; GS, γ-secretase or gamma secretase; GS*i*, γ-secretase inhibitor; HATU, 1-[bis(dimethylamino)methylene]-1*H*-1,2,3-triazolo[4,5-*b*]pyridinium 3-oxide hexafluorophosphate; HCl, hydrochloric acid; K_2CO_3, potassium carbonate; MW, microwave; $NaCNBH_3$, sodium cyanoborohydride; $Pd(PPh_3)_4$, tetrakis(triphenylphosphine)palladium(0); pGP, p-glycoprotein; TFA, trifluoroacetic acid; THF, tetrahydrofuran

■ REFERENCES

(1) Younkin, S. G. The role of Aβ42 in Alzheimer's disease. *J. Physiol.* **1998**, *92*, 289−292.

(2) Kuperstein, I.; Broersen, K.; Benilova, I.; Rozenski, J.; Jonckheere, W.; Debulpaep, M.; Vandersteen, A.; Segers-Nolten, I.; Van Der Werf, K.; Subramaniam, V.; Braeken, D.; Callewaert, G.; Bartic, C.; D'Hooge, R.; Martins, I. C.; Rousseau, F.; Schymkowitz, J.; De Strooper, B. Neurotoxicity of Alzheimer's disease Aβ peptides is induced by small changes in the Aβ42 to Aβ40 ratio. *EMBO J.* **2010**, *29*, 3408−3420.

(3) Hardy, J.; Selkoe, D. J. The amyloid hypothesis of Alzheimer's disease: progress and problems on the road to therapeutics. *Science* **2002**, *297*, 353−356.

(4) Golde, T. E.; Eckman, C. B.; Younkin, S. G. Biochemical detection of Aβ isoforms: implications for pathogenesis, diagnosis, and treatment of Alzheimer's disease. *Biochim. Biophys. Acta, Mol. Basis Dis.* **2000**, *1502*, 172−187.

(5) Haass, C. Take five-BACE and the γ-secretase quartet conduct Alzheimer's amyloid β-peptide generation. *EMBO J.* **2004**, *23*, 483−488.

(6) Annaert, W.; De Strooper, B. A cell biological perspective on Alzheimer's disease. *Annu. Rev. Cell Dev. Biol.* **2002**, *18*, 25−51.

(7) Nikolaev, A.; McLaughlin, T.; O'Leary, D. D. M.; Tessier-Lavigne, M. APP binds DR6 to trigger axon pruning and neuron death via distinct caspases. *Nature* **2009**, *457*, 981−989.

(8) Lauritzen, I.; Pardossi-Piquard, R.; Bourgeois, A.; Pagnotta, S.; Biferi, M.-G.; Barkats, M.; Lacor, P.; Klein, W.; Bauer, C.; Checler, F. Intraneuronal aggregation of the β-CTF fragment of APP (C99) induces Aβ-independent lysosomal-autophagic pathology. *Acta Neuropathol.* **2016**, *132*, 257−276.

(9) Cai, H.; Wang, Y.; McCarthy, D.; Wen, H.; Borchelt, D. R.; Price, D. L.; Wong, P. C. BACE1 is the major β-secretase for generation of Aβ peptides by neurons. *Nat. Neurosci.* **2001**, *4*, 233−234.

(10) Capdeville, R.; Buchdunger, E.; Zimmermann, J.; Matter, A. Glivec (STI571, imatinib), a rationally developed, targeted anticancer drug. *Nat. Rev. Drug Discovery* **2002**, *1*, 493−502.

(11) Cohen, M. H.; Williams, G.; Johnson, J. R.; Duan, J.; Gobburu, J.; Rahman, A.; Benson, K.; Leighton, J.; Kim, S. K.; Wood, R.; Rothmann, M.; Chen, G.; U, K. M.; Staten, A. M.; Pazdur, R. Approval summary for imatinib mesylate capsules in the treatment of chronic myelogenous leukemia. *Clin. Cancer Res.* **2002**, *8*, 935−942.

(12) Dagher, R.; Cohen, M.; Williams, G.; Rothmann, M.; Gobburu, J.; Robbie, G.; Rahman, A.; Chen, G.; Staten, A.; Griebel, D.; Pazdur, R. Approval summary: Imatinib mesylate in the treatment of metastatic and/or unresectable malignant gastrointestinal stromal tumors. *Clin Cancer Res* **2002**, *8*, 3034−3038.

(13) Netzer, W. J.; Dou, F.; Cai, D.; Veach, D.; Jean, S.; Li, Y.; Bornmann, W. G.; Clarkson, B.; Xu, H.; Greengard, P. Gleevec inhibits -amyloid production but not Notch cleavage. *Proc. Natl. Acad. Sci. U.S.A.* **2003**, *100*, 12444−12449.

(14) Netzer, W. J.; Bettayeb, K.; Sinha, S. C.; Flajolet, M.; Greengard, P.; Bustos, V. Gleevec shifts APP processing from a β-cleavage to a nonamyloidogenic cleavage. *Proc. Natl. Acad. Sci. U.S.A.* **2017**, *114*, 1389−1394.

(15) Henley, D. B.; Sundell, K. L.; Sethuraman, G.; Dowsett, S. A.; May, P. C. Safety profile of semagacestat, a gamma-secretase inhibitor: IDENTITY trial findings. *Curr. Med. Res. Opin.* **2014**, *30*, 2021−2032.

(16) Cummings, J. L.; Morstorf, T.; Zhong, K. Alzheimer's disease drug-development pipeline: few candidates, frequent failures. *Alzheimer's Res. Ther.* **2014**, *6*, 37.

(17) Harrison, R. K. Phase II and phase III failures: 2013-2015. *Nat. Rev. Drug Discovery* **2016**, *15*, 817−818.

(18) Godyń, J.; Jończyk, J.; Panek, D.; Malawska, B. Therapeutic strategies for Alzheimer's disease in clinical trials. *Pharmacol. Rep.* **2016**, *68*, 127−138.

(19) Zuhl, A. M.; Nolan, C. E.; Brodney, M. A.; Niessen, S.; Atchison, K.; Houle, C.; Karanian, D. A.; Ambroise, C.; Brulet, J. W.; Beck, E. M.; Doran, S. D.; O'Neill, B. T.; Am Ende, C. W.; Chang, C.; Geoghegan, K. F.; West, G. M.; Judkins, J. C.; Hou, X.; Riddell, D. R.; Johnson, D. S. Chemoproteomic profiling reveals that cathepsin D off-target activity drives ocular toxicity of β−secretase inhibitors. *Nat. Commun.* **2016**, *7*, 13042.

DOI: 10.1021/acs.jmedchem.8b02007
J. Med. Chem. XXXX, XXX, XXX−XXX

(20) Dai, H.; Marbach, P.; Lemaire, M.; Hayes, M.; Elmquist, W. F. Distribution of STI-571 to the brain is limited by P-glycoprotein-mediated efflux. *J Pharmacol Exp Ther* **2003**, *304*, 1085−92.
(21) Breedveld, P.; Pluim, D.; Cipriani, G.; Wielinga, P.; van Tellingen, O.; Schinkel, A. H.; Schellens, J. H. M. The effect of Bcrp1 (Abcg2) on the in vivo pharmacokinetics and brain penetration of Imatinib mesylate (Gleevec): Implications for the use of breast cancer resistance protein and P-glycoprotein inhibitors to enable the brain penetration of imatinib in patients. *Cancer Res.* **2005**, *65*, 2577−2582.
(22) Arslanova, D.; Yang, T.; Xu, X.; Wong, S. T.; Augelli-Szafran, C. E.; Xia, W. Phenotypic analysis of images of zebrafish treated with Alzheimer's gamma-secretase inhibitors. *BMC Biotechnol.* **2010**, *10*, 24.
(23) Raub, T. J. P-Glycoprotein recognition of substrates and circumvention through rational drug design. *Mol. Pharm.* **2006**, *3*, 3−25.
(24) Deadman, B. J.; Hopkin, M. D.; Baxendale, I. R.; Ley, S. V. The synthesis of Bcr-Abl inhibiting anticancer pharmaceutical agents imatinib, nilotinib and dasatinib. *Org. Biomol. Chem.* **2013**, *11*, 1766−1800.
(25) Miyaura, N.; Suzuki, A. Palladium-catalyzed cross-coupling reactions of organoboron compounds. *Chem. Rev.* **1995**, *95*, 2457−2483.
(26) Martin, R.; Buchwald, S. L. Palladium-catalyzed Suzuki−Miyaura cross-coupling reactions employing dialkylbiaryl phosphine ligands. *Acc. Chem. Res.* **2008**, *41*, 1461−1473.
(27) Whelligan, D. K.; Thomson, D. W.; Taylor, D.; Hoelder, S. Two-step synthesis of aza- and diazaindoles from chloroamino-N-heterocycles using ethoxyvinylborolane. *J. Org. Chem.* **2010**, *75*, 11−15.
(28) Bihorel, S.; Camenisch, G.; Lemaire, M.; Scherrmann, J.-M. Influence of breast cancer resistance protein (Abcg2) and P-glycoprotein (Abcb1a) on the transport of imatinib mesylate (Gleevec) across the mouse blood-brain barrier. *J. Neurochem.* **2007**, *102*, 1749−1757.
(29) Netzer, W. J.; Powell, C.; Nong, Y.; Blundell, J.; Wong, L.; Duff, K.; Flajolet, M.; Greengard, P. Lowering β-amyloid levels rescues learning and memory in a down syndrome mouse model. *PLoS One* **2010**, *5*, No. e10943.
(30) Jonsson, T.; Atwal, J. K.; Steinberg, S.; Snaedal, J.; Jonsson, P. V.; Bjornsson, S.; Stefansson, H.; Sulem, P.; Gudbjartsson, D.; Maloney, J.; Hoyte, K.; Gustafson, A.; Liu, Y.; Lu, Y.; Bhangale, T.; Graham, R. R.; Huttenlocher, J.; Bjornsdottir, G.; Andreassen, O. A.; Jönsson, E. G.; Palotie, A.; Behrens, T. W.; Magnusson, O. T.; Kong, A.; Thorsteinsdottir, U.; Watts, R. J.; Stefansson, K. A mutation in APP protects against Alzheimer's disease and age-related cognitive decline. *Nature* **2012**, *488*, 96−99.
(31) Li, D.; Edward, H. K.; Xuewen JoAnn, M.; Youping, H.; Guy, T. C. Applications of high throughput microsomal stability assay in drug discovery. *Comb. Chem. High Throughput Screening* **2008**, *11*, 469−476.
(32) Dahal, U. P.; Jones, J. P.; Davis, J. A.; Rock, D. A. Small molecule quantification by liquid chromatography-mass spectrometry for metabolites of drugs and drug candidates. *Drug Metab. Dispos.* **2011**, *39*, 2355−2360.
(33) Paniagua, R. T.; Sharpe, O.; Ho, P. P.; Chan, S. M.; Chang, A.; Higgins, J. P.; Tomooka, B. H.; Thomas, F. M.; Song, J. J.; Goodman, S. B.; Lee, D. M.; Genovese, M. C.; Utz, P. J.; Steinman, L.; Robinson, W. H. Selective tyrosine kinase inhibition by imatinib mesylate for the treatment of autoimmune arthritis. *J. Clin. Invest.* **2006**, *116*, 2633−2642.
(34) Garcia-Alloza, M.; Robbins, E. M.; Zhang-Nunes, S. X.; Purcell, S. M.; Betensky, R. A.; Raju, S.; Prada, C.; Greenberg, S. M.; Bacskai, B. J.; Frosch, M. P. Characterization of amyloid deposition in the APPswe/PS1dE9 mouse model of Alzheimer disease. *Neurobiol. Dis.* **2006**, *24*, 516−524.
(35) Izco, M.; Pesini, P.; Pérez-Grijalba, V.; Fandos, N.; Sarasa, M. Optimized protocol for amyloid-β extraction from the brain. *J. Alzheimer's Dis.* **2013**, *34*, 835−839.
(36) Nebot, N.; Crettol, S.; d'Esposito, F.; Tattam, B.; Hibbs, D. E.; Murray, M. Participation of CYP2C8 and CYP3A4 in the N-demethylation of imatinib in human hepatic microsomes. *Br. J. Pharmacol.* **2010**, *161*, 1059−1069.
(37) Jack, C. R.; Knopman, D. S.; Jagust, W. J.; Petersen, R. C.; Weiner, M. W.; Aisen, P. S.; Shaw, L. M.; Vemuri, P.; Wiste, H. J.; Weigand, S. D.; Lesnick, T. G.; Pankratz, V. S.; Donohue, M. C.; Trojanowski, J. Q. Tracking pathophysiological processes in Alzheimer's disease: an updated hypothetical model of dynamic biomarkers. *Lancet Neurol.* **2013**, *12*, 207−216.
(38) Guerreiro, R.; Bras, J. The age factor in Alzheimer's disease. *Genome Med.* **2015**, *7*, 106.
(39) Rodrigue, K. M.; Kennedy, K. M.; Devous, M. D.; Rieck, J. R.; Hebrank, A. C.; Diaz-Arrastia, R.; Mathews, D.; Park, D. C. β-Amyloid burden in healthy aging: Regional distribution and cognitive consequences. *Neurology* **2012**, *78*, 387−395.
(40) Davis, D. G.; Schmitt, F. A.; Wekstein, D. R.; Markesbery, W. R. Alzheimer neuropathologic alterations in aged cognitively normal subjects. *J. Neuropathol. Exp. Neurol.* **1999**, *58*, 376−388.
(41) Bennett, D. A.; Schneider, J. A.; Arvanitakis, Z.; Kelly, J. F.; Aggarwal, N. T.; Shah, R. C.; Wilson, R. S. Neuropathology of older persons without cognitive impairment from two community-based studies. *Neurology* **2006**, *66*, 1837−1844.
(42) Gardner, L. E.; White, J. D.; Eimerbrink, M. J.; Boehm, G. W.; Chumley, M. J. Imatinib methanesulfonate reduces hyperphosphorylation of tau following repeated peripheral exposure to lipopolysaccharide. *Neuroscience* **2016**, *331*, 72−77.
(43) Cancino, G. I.; Toledo, E. M.; Leal, N. R.; Hernandez, D. E.; Yévenes, L. F.; Inestrosa, N. C.; Alvarez, A. R. STI571 prevents apoptosis, tau phosphorylation and behavioural impairments induced by Alzheimer's β-amyloid deposits. *Brain* **2008**, *131*, 2425−2442.
(44) Vassar, R. BACE1 inhibitor drugs in clinical trials for Alzheimer's disease. *Alzheimer's Res. Ther.* **2014**, *6*, 89.
(45) Yan, R. Physiological functions of the beta-site amyloid precursor protein cleaving enzyme 1 and 2. *Front. Mol. Neurosci.* **2017**, *10*, 97.
(46) Jester, B. W.; Cox, K. J.; Gaj, A.; Shomin, C. D.; Porter, J. R.; Ghosh, I. A coiled-coil enabled split-luciferase three-hybrid system: applied toward profiling inhibitors of protein kinases. *J. Am. Chem. Soc.* **2010**, *132*, 11727−11735.

DOI: 10.1021/acs.jmedchem.8b02007
J. Med. Chem. XXXX, XXX, XXX−XXX